Article ID: 1006-8775(2009) 01-0167-14

DEFORMATION OF MOISTURE FLUX CIRCULATION SURROUNDING THE LANDFALL TYPHOON "BILIS"

RAN Ling-kun (冉令坤)[1], YANG Wen-xia (杨文霞)[1, 2], HONG Yan-chao (洪延超)[1]

(1. Institute of Atmospheric Physics, Chinese Academy of Sciences, Beijing 100029 China; 2. Graduate School of Chinese Academy of Sciences, Beijing 100049 China)

Abstract: The deformation parameter (DP), which is defined as the product of shear deformation and stretching deformation of moisture flux circulation, is introduced. The tendency equation of DP is derived in pressure coordinates. Furthermore, DP is used to diagnose the deformation character of moisture flux circulation in the periphery of Bilis. The analysis showed that before Bilis landed, DP presented eight abnormal areas, which distributed alternately and closely encircled the low-pressure center. This indicated that the moisture flux circulation in the periphery of Bilis rotated counterclockwise and stretched longitudinally and latitudinally to deform. After Bilis landed, DP weakened gradually and its regular pattern of horizontal distribution loosened. The shear and stretching deformations of moisture flux circulation surrounding Bilis weakened after the typhoon landed. The deformation of moisture flux circulation in the periphery of Bilis mainly appeared in the middle-lower troposphere. There existed 1/2 phase difference between the shear and stretching deformations in the vertical-latitudinal cross section and a $\frac{\pi}{4}$ phase difference between them on the horizontal plane. As Bilis landed and further moved inland of China, the intensities of DP, shear and stretching deformations decreased, meanwhile their vertical and horizontal structures became irregular. The chief dynamic factors responsible for the deformation of moisture flux circulation in the periphery of Bilis were the three terms associated with the three-dimensional advection transportation of DP, square difference between shear and stretching deformations coupling with Coriolis parameter, and horizontal gradient of geopotential height before Bilis landed. The last two dynamic factors impacted jointly on the deformation of moisture flux circulation after Bilis landed.

Key words: deformation parameter; shear deformation; stretching deformation; moisture flux circulation

CLC number: P457.6 **Document code:** A **doi:** 10.3969/j.issn.1006-8775.2009.02.006

1 INTRODUCTION

As wind is one of the most fundamental meteorological elements, its significance goes without saying. The horizontal wind field can be decomposed into four parts: advection, rotation, divergence, and deformation[1-3]. Vorticity and divergence are widely used to diagnose dynamic characteristics of atmospheric motion and analyze the evolution of synoptic systems. However, besides rotation and divergence, deformation is also one of the features of atmospheric flow. Compared with the frequent use of vorticity and divergence, studies involving the deformation field have been relatively less, though its role in atmospheric motion is attracting more and more attention. Zhang [4] and Deng [5] indicated that changes in the deformation field were closely related to severe rainstorms, so that it can be used to judge the movement and development of low-pressure systems and might serve as a indicator for 12- and 24-hour heavy rainfall. Martin [6] analyzed the deformation term in the quasigeostrophic (QG) omega equation and concluded that the deformation term played an important role in the middle troposphere when a cyclone approached its post-maturity stage. Wang and Wu [7] discussed the development of symmetric disturbances in a baroclinic frontal zone under the condition of deformation frontogenesis. Han et al. [8] found that the deformation term in the traditional

Received date: 2009-03-28; **revised date:** 2009-09-04
Foundation item: National Basic Research Program of China (2009CB421505); National Natural Sciences Foundations of China (40875032 and 40875002); Major Foreland Project of IAP (IAP07201)
Biography: RAN Ling-kun, PhD, mainly undertaking the research on tropical cyclones and mesoscale dynamics.
E-mail for correspondence author: rlk@mail.iap.ac.cn

frontogenesis function played a more important role than the divergence term and "dip" term and had a serious influence on the extratropical transformation of typhoons. Li and Colucci [9] stated that the interaction between deformation and potential vorticity was one of the vital mechanisms leading to the onset of blocking in the Southern Hemisphere. The results of Liu et al. [10] showed that the flow of lower-level high pressure was linked with not only clockwise rotational deformation but also divergent deformation, when friction was considered. Furthermore, only the deformation field can be found around the saddle point of standard saddle fields. Gao et al. [11, 12] defined the absolute value of the horizontal gradient of bulk deformation as the general frontogenesis function. Diagnostic analysis indicated that the confluence of the deformation field and water vapor transport by deformation flow were favorable for the development of heavy-rainfall events.

Previous studies on deformation highlighted the effect of deformation on the physical mechanisms of weather events. However, the diagnostic analysis of the deformation characteristics of atmospheric flow itself, especially for cyclonic flow surrounding typhoons, is not sufficient. Thus, the purpose of this paper is to introduce a concept of deformation parameter (DP) to diagnose the deformation character of atmospheric flow on the basis of previous investigations. In the next section, the deformation parameter for moisture flux circulation is introduced and its physical meaning is given. In the third section, DP is applied to investigate the deformation characteristics of the moisture flux circulation surrounding the low-pressure center of Typhoon Bilis and the primary dynamic factors responsible for the development of DP are analyzed. The summary is given in the fourth section.

2 DEFORMATION PARAMETER

According to Petterssen [13] and Gao [12], the horizontal moisture flux can be approximately written as

$$u_{q_v} = u_{q_v 0} + \left(D + \eta_{q_v}\right)\frac{x}{2} + \left(\zeta_{q_v} - \xi\right)\frac{y}{2}, \qquad (1)$$

$$v_{q_v} = v_{q_v 0} + \left(\zeta_{q_v} + \xi\right)\frac{x}{2} + \left(D - \eta_{q_v}\right)\frac{y}{2}, \qquad (2)$$

where $\left(u_{q_v},\ v_{q_v}\right) = \left(uq_v,\ vq_v\right)$ is the horizontal moisture flux (referred to as "moisture flux" hereafter), with $\left(u,\ v\right)$ the horizontal wind vector, q_v the specific humidity, and $\left(u_{q_v 0},\ v_{q_v 0}\right)$ the moisture flux at the origin of coordinates. In the above two expressions,

$D = \frac{\partial u_{q_v}}{\partial x} + \frac{\partial v_{q_v}}{\partial y}$, $\xi = \frac{\partial v_{q_v}}{\partial x} - \frac{\partial u_{q_v}}{\partial y}$, $\eta_{q_v} = \frac{\partial u_{q_v}}{\partial x} - \frac{\partial v_{q_v}}{\partial y}$, $\zeta_{q_v} = \frac{\partial v_{q_v}}{\partial x} + \frac{\partial u_{q_v}}{\partial y}$ represent the horizontal divergence, relative vertical vorticity, stretching deformation, and shear deformation, respectively.

Petterssen [13] and Gao et al. [11] introduced the bulk deformation, defined as $E = \left({\zeta_{q_v}}^2 + {\eta_{q_v}}^2\right)^{1/2}$ to describe the horizontal deformation of the flow. Its advantage is that the value of E does not vary as the coordinates rotate. Here, a new scalar deformation parameter (DP) is adopted, which is defined as the product of shear deformation and stretching deformation, to represent the deformation characteristics of the moisture flux circulation. Thus, DP is given by

$$H_{q_v} = \zeta_{q_v}\eta_{q_v} = \left(\frac{\partial v_{q_v}}{\partial x} + \frac{\partial u_{q_v}}{\partial y}\right)\left(\frac{\partial u_{q_v}}{\partial x} - \frac{\partial v_{q_v}}{\partial y}\right). \qquad (3)$$

It is clear that DP reflects the synthetic character of stretching and shear deformations of moisture flux. The physical significance of DP may be essentially interpreted by considering, for example, an idealized two-dimensional flow. As shown in Fig. 1a, the asymptotes of streamlines associated with shear deformation (ζ_{q_v}) form a 45-degree angle with the coordinate axis. ζ_{q_v} is anomalous in the four areas divided by the two orthogonal asymptotes. In areas Ⅰ and Ⅲ of Fig. 1a, if moisture flux gradually approaches the y' axis, $\zeta_{q_v} = \frac{\partial v_{q_v}}{\partial x} + \frac{\partial u_{q_v}}{\partial y} > 0$ due to $\frac{\partial v_{q_v}}{\partial x} < 0$, $\frac{\partial u_{q_v}}{\partial y} > 0$, and $\delta x > \delta y$. This indicates that moisture flux circulation in areas Ⅰ and Ⅲ is rotated counterclockwise to deform toward the y' axis. In areas Ⅱ and Ⅳ of Fig. 1a, if moisture flux gradually approaches the x' axis, $\zeta_{q_v} = \frac{\partial v_{q_v}}{\partial x} + \frac{\partial u_{q_v}}{\partial y} < 0$ due to $\frac{\partial v_{q_v}}{\partial x} < 0$, $\frac{\partial u_{q_v}}{\partial y} > 0$ and $\delta x < \delta y$. This indicates that moisture flux circulation in areas Ⅱ and Ⅳ rotates counterclockwise to deform toward the x' axis. As shown in Fig. 1b, the asymptotes of streamlines of stretching deformation (η_{q_v}) are parallel to the coordinate axis. The anomalies of η_{q_v} are mainly located in the four quadrants. In areas Ⅰ and Ⅲ of Fig. 1b, if moisture

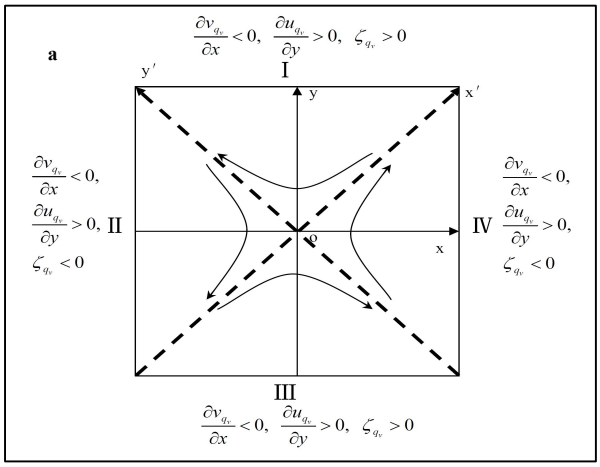

Fig.1 Horizontal distribution schematic diagrams of shear deformation ζ_{q_v} (a), stretching deformation η_{q_v} (b), and deformation parameter H_{q_v} (c).

flux gradually approaches the x axis, $\eta_{q_v}=\dfrac{\partial u_{q_v}}{\partial x}-\dfrac{\partial v_{q_v}}{\partial y}>0$ due to $\dfrac{\partial u_{q_v}}{\partial x}>0$ and $\dfrac{\partial v_{q_v}}{\partial y}<0$, which indicates that the moisture flux circulation in areas Ⅰ and Ⅲ extends along the x axis but contracts along the y axis. In areas Ⅱ and Ⅳ of Fig. 1b, if moisture flux gradually approaches the y axis, $\eta_{q_v}=\dfrac{\partial u_{q_v}}{\partial x}-\dfrac{\partial v_{q_v}}{\partial y}<0$ due to $\dfrac{\partial u_{q_v}}{\partial x}<0$ and $\dfrac{\partial v_{q_v}}{\partial y}>0$, which indicates that the moisture flux circulation in areas Ⅱ and Ⅳ contracts along the x axis but extends along the y axis. DP (H_{q_v}) is the coupling of shear deformation with stretching deformation. As shown by Fig. 1c, since the phase difference between ζ_{q_v} and η_{q_v} is $\dfrac{\pi}{4}$, H_{q_v} represents the eight anomalous areas that alternate in positive and negative values. This indicates that the moisture flux circulation in areas Ⅰ, Ⅳ, Ⅴ, and Ⅷ rotates counterclockwise and deforms to expand zonally. Meanwhile, the moisture flux circulation in areas Ⅱ, Ⅲ, Ⅵ, and Ⅶ rotates counterclockwise and deforms to expand meridionally.

We will use DP to analyze the deformation characteristics of the moisture flux circulation in the periphery of Bilis. The moisture flux circulation surrounding the typhoon is typically cyclonic, whose deformation is noticeable and varies as well as its rotation and divergence. So the spatial distribution and the temporal evolution of DP for Bilis will be diagnosed in the following section.

At the same time, in order to further investigate the main dynamic factors responsible for the deformation of the moisture flux circulation surrounding Bilis, the tendency equation of DP is derived from primitive equations in pressure coordinates. The equations of motion, continuity, thermodynamics, state, and water vapor are given by

$$\frac{du}{dt}-fv=-\frac{\partial\phi}{\partial x}, \tag{4}$$

$$\frac{dv}{dt}+fu=-\frac{\partial\phi}{\partial y}, \tag{5}$$

$$\frac{\partial\phi}{\partial p}=-\frac{1}{\rho}, \tag{6}$$

$$\nabla\cdot\mathbf{v}=0, \tag{7}$$

$$\frac{d\theta}{dt}=S_\theta, \tag{8}$$

$$p=\rho RT\left(1+\lambda q_v\right), \tag{9}$$

$$\frac{dq_v}{dt} = S_{q_v}, \tag{10}$$

where S_θ and S_{q_v} are the sources or sinks of θ and q_v, respectively, and the other symbols have their usual meteorological definitions. Combining the above equations, one may easily obtain the tendency equation of DP.

$$\begin{aligned}\frac{\partial H_{q_v}}{\partial t} = & \underbrace{-\mathbf{v}\cdot\nabla H_{q_v}}_{H_{q_v}1} + \underbrace{f\left(\zeta_{q_v}{}^2 - \eta_{q_v}{}^2\right)}_{H_{q_v}2} + \underbrace{\frac{\partial w}{\partial y}\left(\frac{\partial v_{q_v}}{\partial p}\zeta_{q_v} - \frac{\partial u_{q_v}}{\partial p}\eta_{q_v}\right) - \frac{\partial w}{\partial x}\left(\frac{\partial u_{q_v}}{\partial p}\zeta_{q_v} + \frac{\partial v_{q_v}}{\partial p}\eta_{q_v}\right)}_{H_{q_v}3} \\ & + \underbrace{\left[\begin{array}{l} -\left(\frac{\partial u_{q_v}}{\partial y}\frac{\partial v}{\partial y} + \frac{\partial v_{q_v}}{\partial x}\frac{\partial u}{\partial x} + \frac{\partial v_{q_v}}{\partial y}\frac{\partial v}{\partial x} + \frac{\partial u_{q_v}}{\partial x}\frac{\partial u}{\partial y}\right)\eta_{q_v} + \\ \left(\frac{\partial v_{q_v}}{\partial y}\frac{\partial v}{\partial y} - \frac{\partial u_{q_v}}{\partial y}\frac{\partial v}{\partial x} - \frac{\partial u_{q_v}}{\partial x}\frac{\partial u}{\partial x} + \frac{\partial v_{q_v}}{\partial x}\frac{\partial u}{\partial y}\right)\zeta_{q_v} \end{array}\right]}_{H_{q_v}4} \\ & + \underbrace{\left\{-\left[\frac{\partial}{\partial y}\left(q_v\frac{\partial \phi}{\partial x}\right) + \frac{\partial}{\partial x}\left(q_v\frac{\partial \phi}{\partial y}\right)\right]\eta_{q_v} - \left[\frac{\partial}{\partial x}\left(q_v\frac{\partial \phi}{\partial x}\right) - \frac{\partial}{\partial y}\left(q_v\frac{\partial \phi}{\partial y}\right)\right]\zeta_{q_v}\right\}}_{H_{q_v}5} \\ & + \underbrace{\left(\frac{\partial vS_{q_v}}{\partial x} + \frac{\partial uS_{q_v}}{\partial y}\right)\eta_{q_v} + \left(\frac{\partial uS_{q_v}}{\partial x} - \frac{\partial vS_{q_v}}{\partial y}\right)\zeta_{q_v}}_{H_{q_v}6}\end{aligned} . \tag{11}$$

It can be seen from Eq. (11) that the term on the left-hand side is the local change of DP. The first term on the right-hand side (RHS), namely H_{q_v1}, denotes the three-dimensional spatial advection of DP. The second RHS term, namely H_{q_v2}, is the difference between squared shear and stretching deformations, which coupled with the Coriolis parameter. The third term on the RHS, namely H_{q_v3}, is the distortion term consisting of the horizontal gradient of vertical velocity and the vertical shear of horizontal moisture flux. The fourth term on the RHS, namely H_{q_v4}, stands for the coupling of the horizontal gradients of horizontal momentum and moisture flux with the shear and stretching deformations. The fifth term on the RHS, namely H_{q_v5}, reflects the contribution of the horizontal gradient of geopotential height. The sixth RHS term, namely H_{q_v6}, is the source or sink of DP, reflecting the contribution of horizontal fluxes of sources/sinks of vapor to the local change of DP.

3 DEFORMATION OF MOISTURE FLUX CIRCULATION

3.1 *Overview of Bilis*

Bilis originated from a tropical storm forming over the ocean east of the Philippines early on 9 July 2006. The storm was upgraded to a severe tropical storm (STS) in the afternoon of 11 July. Bilis made landfall in Yilan County of Taiwan province at 2300 UTC 13 July and then entered the Taiwan Strait. At 1250 UTC 14 July, Bilis made landfall once again along the coast of Xiapu County, Fujian province, with maximum surface velocity of 30 m s^{-1}. After landfall, Bilis continued to move northwestwards and arrived in the southwest of Jiangxi province in the afternoon of July 15 at tropical depression strength. After passing southwestward over Hunan and Guangxi provinces, Bilis dissipated in eastern Yunnan province during the night of July 18.

Jointly influenced by the western Pacific subtropical high, high pressure in the northern mainland, and a lower-latitude equatorial high-pressure circulation, Bilis had been deep into inland for five days. Interacting with a strong, warm, and moist southwesterly flow, Bilis brought heavy rainfall as well as extreme torrential rainfall to most parts of Fujian, Zhejiang, Jiangxi, Hunan, Guangdong, and Guangxi. Precipitation at the levels caused by Bilis has rarely been seen historically, in terms of precipitation intensity, persistence, duration, and horizontal scale.

3.2 *Data and method*

The NCEP/NCAR Global Final Analysis (FNL) dataset, with horizontal resolution of 1°×1°, 26 vertical pressure levels, and a 6-hour time interval, is used. The

deformation parameter (H_{q_v}) and five forcing terms (H_{q_v1}, H_{q_v2}, H_{q_v3}, H_{q_v4} and H_{q_v5}) in Eq. (11) are calculated from the FNL dataset. Due to the lack of suitable data with high temporal resolution for diabatic heating and phase changes of water, the local change of DP and sources/sinks of DP in Eq. (11) are not evaluated here. The significant contributions of this study relate to characterizing the deformation of the moisture flux circulation surrounding Bilis and analyzing the primary dynamic factors responsible for its changes. So the vertical integrations of DP and its forcing terms are used here, with integrals defined by $\langle \bullet \rangle = -\int_{p_s}^{p_t} \bullet dp$, where p_s is the surface pressure and p_t is the top pressure level of the model.

3.3 *Deformation diagnosis*

The horizontal distributions of DP ($\langle H_{q_v} \rangle$) before and after landfall are presented in Fig. 2. As is shown, at 0000 UTC 13 July when the low-pressure center of Bilis was approaching the island of Taiwan, $\langle H_{q_v} \rangle$ presented eight anomalous areas, whose positive values alternated with negatively valued areas closely surrounding the low-pressure center. The horizontal distribution pattern of the eight anomalous areas is relatively regular. The configuration of positively- and negatively-valued areas of DP basically corresponds to the theoretical analysis of Fig. 1c so that the areal designations in Fig. 1c continue to be applicable in the following section. The intensity of $\langle H_{q_v} \rangle$ in areas Ⅰ, Ⅱ, Ⅶ, and Ⅷ is larger than in the other areas. This indicates that the counterclockwise rotation and latitudinal expansion deformations of moisture flux circulation in areas Ⅰ and Ⅷ are relatively remarkable, and so is the counterclockwise rotation and longitudinal expansion deformations of moisture flux circulation in areas Ⅱ and Ⅶ. At 0600 UTC 13 July when the low-pressure center of Bilis at 980 hPa arrived at (23°N, 123°E), the western edge of Bilis grazed Taiwan. The cyclonic moisture flux circulation in the periphery of Bilis was still strong and the horizontal distribution pattern of $\langle H_{q_v} \rangle$ was similar to that of 0000 UTC 13 July. The eight anomalous areas of DP encircled Bilis, which was consistent with Fig. 1c. Compared with the situation at 0000 UTC 13 July, the intensity of each of these eight areas increased, which indicated that the counterclockwise rotation and latitudinal/longitudinal expansion deformations of moisture flux circulation were enhanced together. At 1200 UTC 13 July when the low-pressure center of Bilis made partial landfall on the island of Taiwan, the intensity of DP began to decrease except in area Ⅲ. The positive value of $\langle H_{q_v} \rangle$ in area Ⅲ continued to enhance, indicating that the counterclockwise rotation and longitudinal expansion deformations of moisture flux circulation there were further strengthened. At 1800 UTC 13 July when the low-pressure center of Bilis covered Taiwan and its western edge approached to the Chinese mainland, the intensity of $\langle H_{q_v} \rangle$ in areas Ⅲ and Ⅴ decreased while the intensity of $\langle H_{q_v} \rangle$ in other areas increased, indicating that the counterclockwise rotation shear and stretching deformations of moisture flux circulation in the eastern and northern periphery of Bilis continued to enhance. At 0000 UTC 14 July, the western portion of Bilis made landfall on the southeast coastline of China. Although $\langle H_{q_v} \rangle$ still maintained the previous horizontal distribution pattern, its intensity, especially in the western periphery of Bilis, apparently decreased and was smaller than at 1800 UTC 13 July. At 0600 UTC 14 July when Bilis made landfall, the deformation parameter was further weakened. Accompanying the horizontal-scale enlargement of low-pressure center, the horizontal structure of $\langle H_{q_v} \rangle$ became looser and the areas of anomalous $\langle H_{q_v} \rangle$ extended accordingly. At 1200 UTC 14 July after Bilis made landfall, not only the intensity of $\langle H_{q_v} \rangle$ was further diminished, but also its horizontal distribution pattern became irregular. In addition, the deformation areas of the moisture flux circulation were relatively far from the low-pressure center. This implies that as the cyclonic moisture flux circulation surrounding Bilis weakened, the accompanying deformation decreased. During 1800 UTC 14 – 0000 UTC 15 July, the horizontal range of the low-pressure center shrank suddenly and the structure of the moisture flux circulation surrounding Bilis adjusted. The intensity of $\langle H_{q_v} \rangle$ slightly increased, but its horizontal distribution pattern was still irregular.

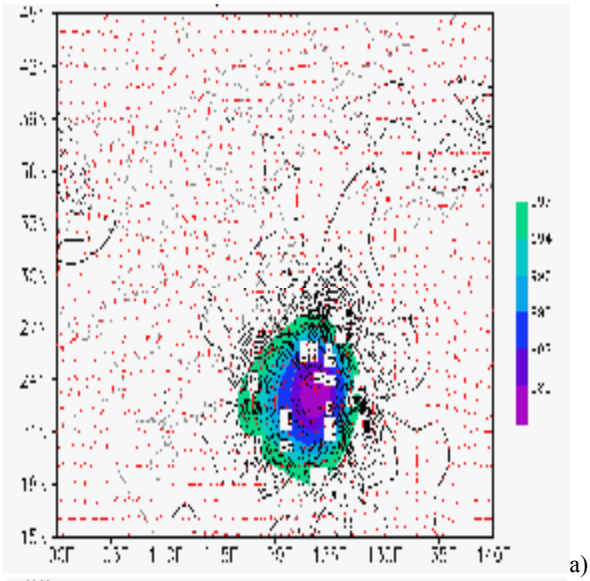
a)

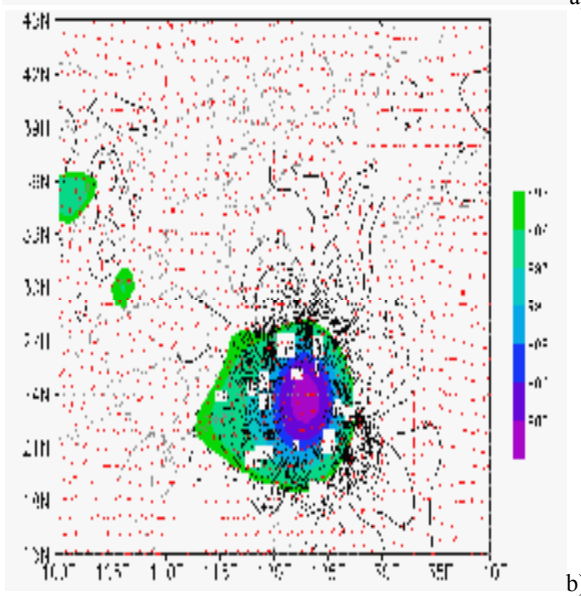
b)

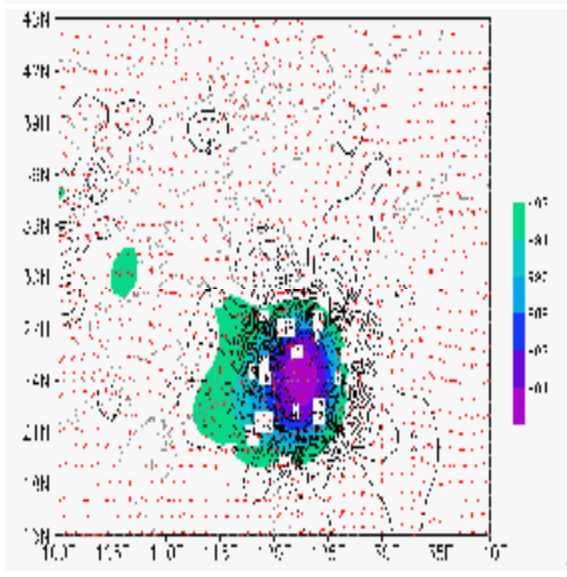
c)

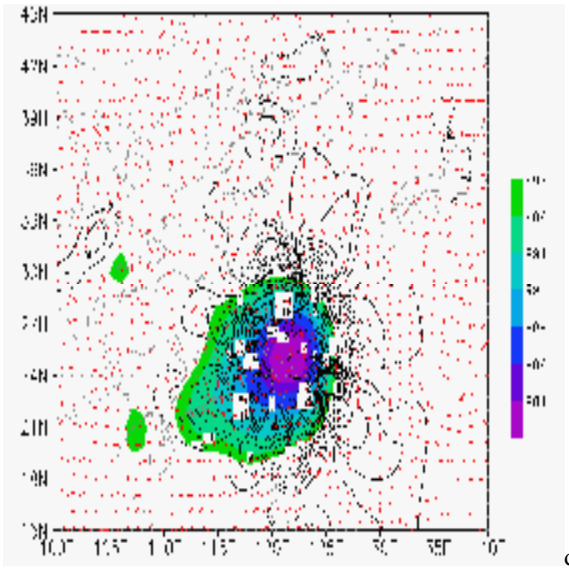
d)

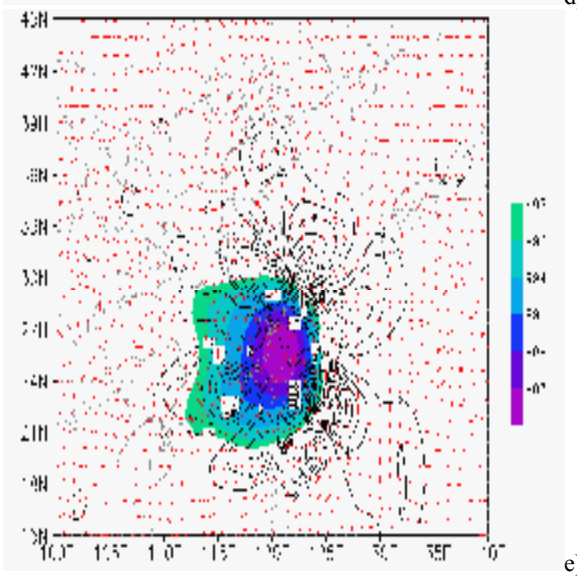
e)

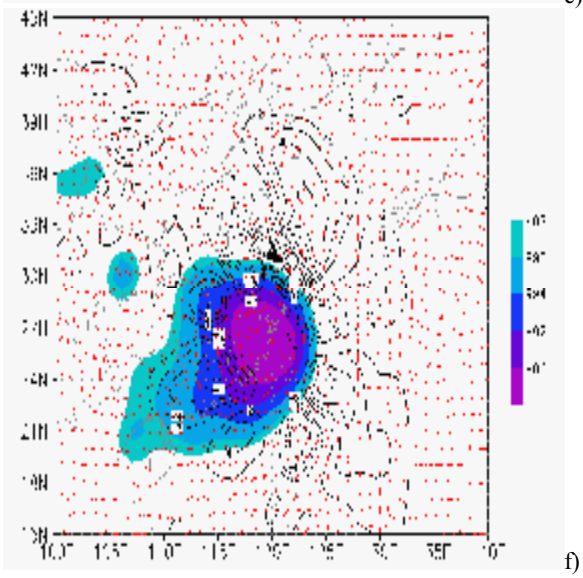
f)

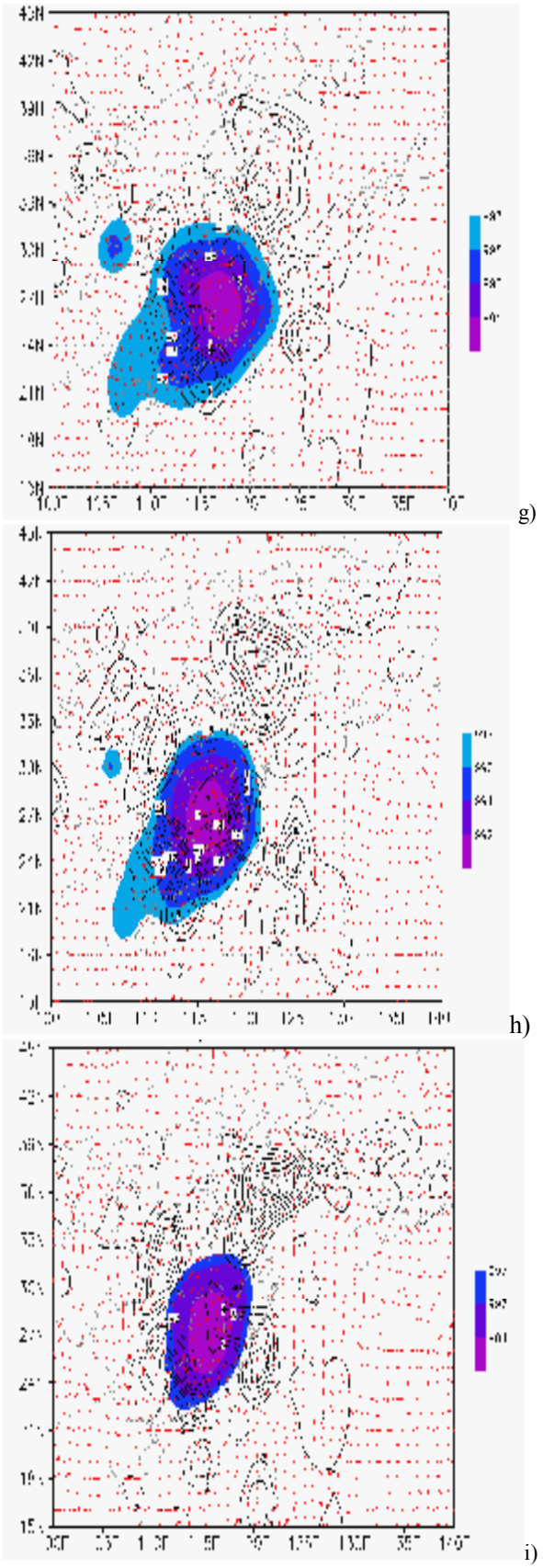

Fig.2 Horizontal distribution of DP vertically integrated ($\langle H_{q_v} \rangle$, Unit: 10^{-9} Pa s^{-2}) at 0000 UTC 13(a), 0600 UTC 13(b), 1200 UTC 13(c), 1800 UTC 13(d), 0000 UTC 14(e), 0600 UTC 14(f), 1200 UTC 14 (g), 1800 UTC 14 (h) and 0000 UTC 15, July 2006(i). The arrow stands for the horizontal wind vector on 850 hPa and the color shade denotes the sea-level pressure. The ordinate is the latitude and the abscissa is the longitude.

From the above analysis of $\langle H_{q_v} \rangle$, it can be seen that before Bilis made landfall, the intensity of DP of the moisture flux circulation in its periphery was strong and had eight areas of anomalies, in which the positive values alternated with negative values, all closely surrounding Bilis. The horizontal distribution pattern of DP was relatively regular. This indicates that the moisture flux circulation in the periphery of Bilis was subjected to counterclockwise rotational shear deformation and longitudinal and latitudinal stretching deformations before landfall. Accompanying the landfall of Bilis, the shape of the moisture flux circulation in the periphery of Bilis varied gradually from the originally nearly circular shape to an elliptical shape, and the intensity of $\langle H_{q_v} \rangle$ decreased coincidently. The horizontal distribution structure of $\langle H_{q_v} \rangle$ also became relatively loose. This meant that the deformation of the moisture flux circulation surrounding Bilis was undermined when the storm made landfall. After Bilis went deep inland, the moisture flux circulation was further damped. The intensity of DP anomalies decreased correspondingly, and the horizontal distribution pattern evolved to be irregular. This indicates that the shear and stretching deformations of moisture flux circulation surrounding Bilis were no longer distinct following the attenuation of Bilis and its circulation.

The vertical distributions of DP (H_{q_v}), shear deformation (ζ_{q_v}), and stretching deformation (η_{q_v}) along the northern periphery of Bilis are presented in Fig. 3. As is shown, at 1200 UTC 13 July before Bilis made landfall, the strongly positive and negative areas of H_{q_v} were tightly adjacent and primarily located in the longitudes of 120°E – 127°E. The anomalous areas of H_{q_v} — with the positive and negative centers appearing at about 975 hPa — extended vertically from the surface layer upwards to 350 hPa. The strongly positive and negative areas of stretching deformation η_{q_v} with two positively- and negatively-valued centers at 900 hPa were located over the longitudes of 119°E – 127°E in the middle-lower troposphere, and the latitudinal scale of η_{q_v} was a little wider than that of H_{q_v}. The anomalous areas of

shear deformation ζ_{q_v} mainly were positive and located over the longitudes of 122°E－126°E in the middle-lower troposphere, with the positive center at 900 hPa. Another remarkable characteristic was that the positive high-valued area of ζ_{q_v} was located in the middle of strongly positive and negative areas of η_{q_v}, meaning that there existed a ½-phase difference between ζ_{q_v} and η_{q_v} in the zonal distribution. At 0000 UTC 14 July when Bilis made landfall, the vertical distributions of structures of DP, stretching deformation, and shear deformation were similar to those at 1200 UTC 13 July. The positive and negative high-valued areas were located in the middle-lower troposphere, and the positive anomaly of ζ_{q_v} lay in the ½-phase location between the positive and negative anomalies of η_{q_v}. But the intensities of H_{q_v}, ζ_{q_v}, and η_{q_v} were weakened, indicating that the counterclockwise rotational deformation, longitudinal stretching deformation, and latitudinal stretching deformation decreased in the northern periphery of Bilis when the typhoon made landfall. At 1200 UTC 14 July after landfall, the shear and stretching deformations of moisture flux circulation surrounding Bilis were weakened further. The four positive- and negative-valued areas of H_{q_v} appeared over the longitudes of 110°E－130°E below the 800 hPa level, with relatively loose latitudinal distribution. Although the intensities of the four anomalous areas of H_{q_v} were almost equal to each other, they were weaker than those at 0000 UTC 14 July. ζ_{q_v} was located in the ½-phase location relative to the extrema of η_{q_v}. The latitudinal width of the two deformations became wider, but their intensity was obviously lessened.

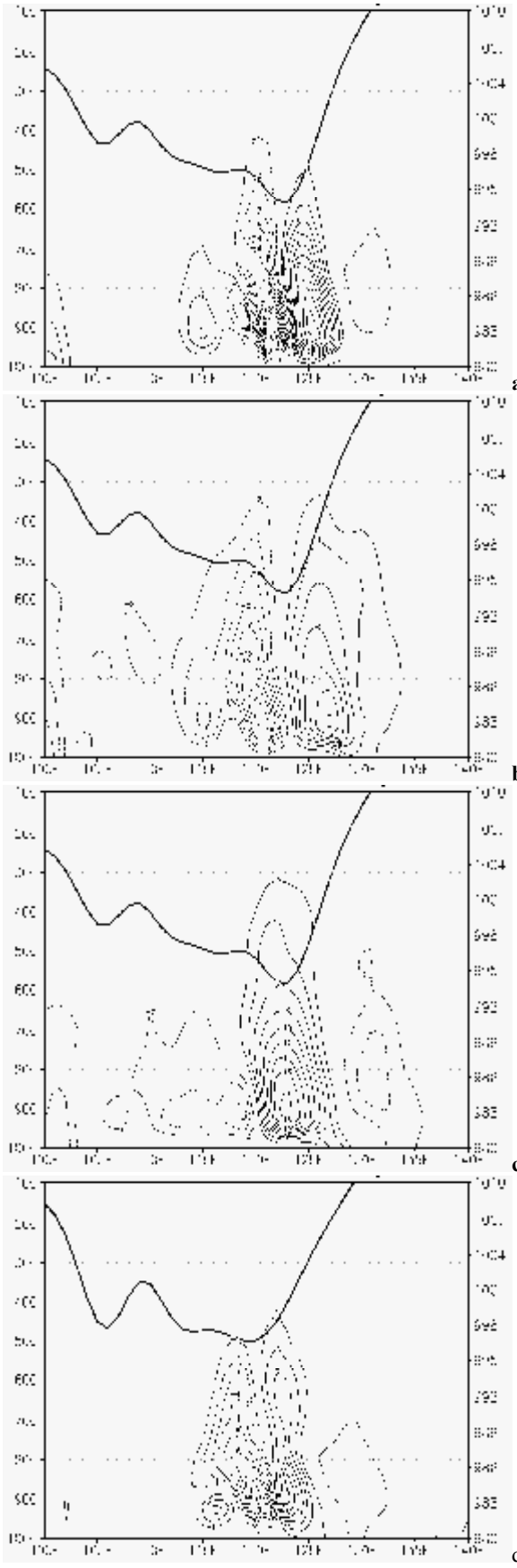

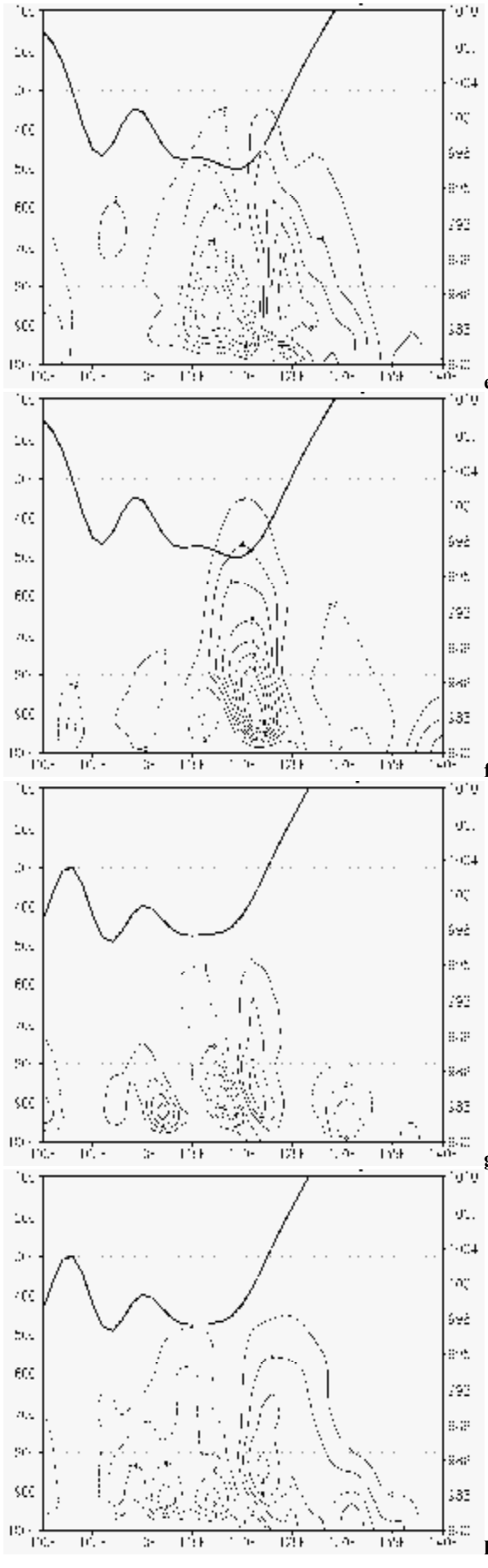

Fig.3 Vertical-latitudinal cross sections at 1200 UTC 13 (a, b, c along 28°N) , 0000 UTC 14 (d, e, f along 30°N) and 1200 UTC 14, July 2006 (g, h, i along 32°N) of deformation parameter H_{q_v} (a, d, g, Unit: 10^{-13} s^{-2}), stretching deformation η_{q_v} (b, e, h, Unit: 10^{-7} s^{-1}) and shear deformation ζ_{q_v} (c, f, i, Unit: 10^{-7} s^{-1}). The thick solid line denotes the sea-level pressure. The ordinate is the pressure in hPa and the abscissa is the longitude in degree.

The horizontal distributions of DP, stretching deformation, and shear deformation at 850 hPa are presented in Fig. 4. As is shown, at 1200 UTC 13 July before landfall, the eight anomalous areas of H_{q_v}, in which the positive-valued areas alternated with the negative-valued areas, were located in the periphery of Bilis and encircled the low-pressure center. The horizontal distribution pattern of H_{q_v} was consistent with the theoretical analysis based on Fig. 1c. η_{q_v} appeared in the four anomalous areas that were symmetrically distributed around the eye of Bilis. The two positively-valued areas of η_{q_v} were located in the northeastern and southwestern periphery regions of Bilis, respectively, indicating that the moisture flux circulation there extended latitudinally and contracted longitudinally. The two negatively-valued areas of η_{q_v} appeared along the northwestern and southeastern periphery of Bilis, indicating that the moisture flux circulation there extended longitudinally and contracted latitudinally. The distribution pattern of η_{q_v} basically corresponded to the theoretical analysis of Fig. 1b. The anomalous areas of ζ_{q_v} were the four positively- and negatively-valued areas that were alternately distributed around the low-pressure center of Bilis. ζ_{q_v} along the northern and southern periphery of Bilis

were positive, indicating that the moisture flux circulation there rotated counterclockwise towards the northeast and southwest respectively to deform. ζ_{q_v} was negative along the eastern and western edges of Bilis, indicating that the moisture flux circulation there rotated counterclockwise towards the northwest and southeast respectively to deform. The horizontal distribution pattern of ζ_{q_v} was basically in accordance with the theoretical analysis in Fig. 1a. Thus, it could be inferred that there existed a $\frac{\pi}{4}$ phase difference between the horizontal distributions of η_{q_v} and ζ_{q_v}. With Bilis making landfall and going deep inland, the intensity of H_{q_v} surrounding Bilis was reduced, and its regular horizontal distribution pattern was also destroyed gradually. Although the horizontal distribution patterns of η_{q_v} and ζ_{q_v} stayed relatively regular until Bilis went deeper inland, the intensities decreased gradually, indicating that their temporal evolution was similar to that of H_{q_v}.

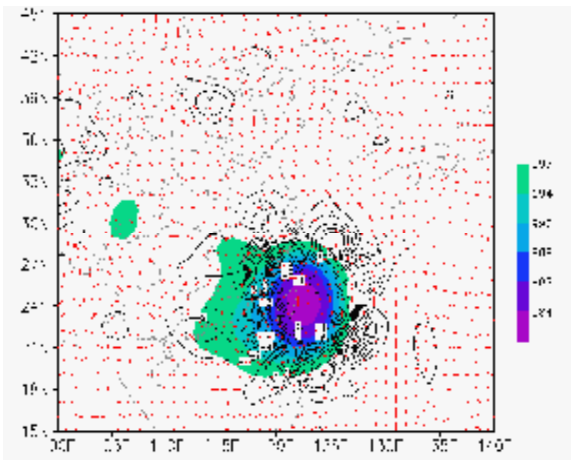
a)

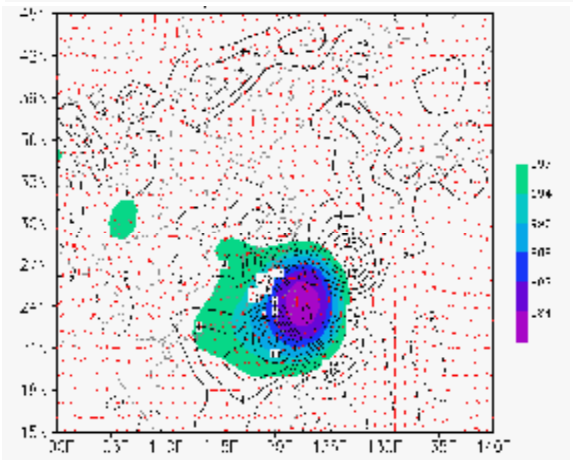
b)

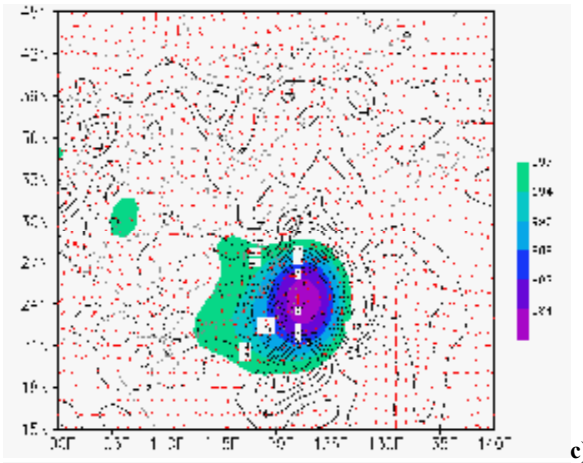
c)

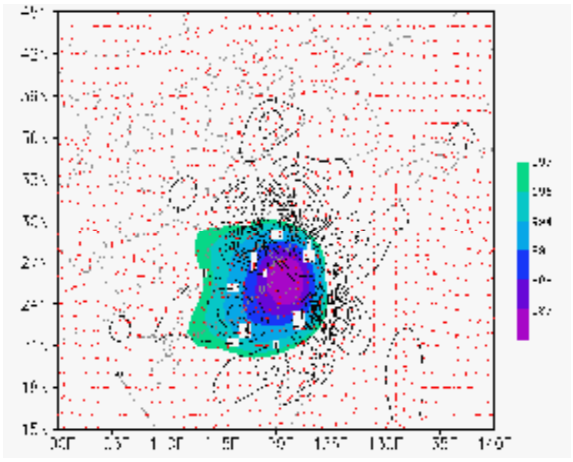
d)

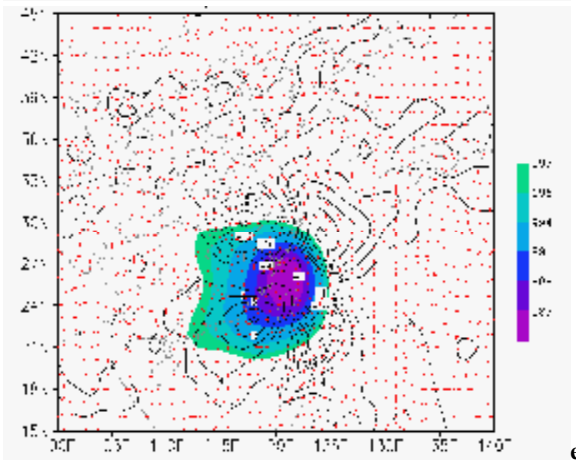
e)

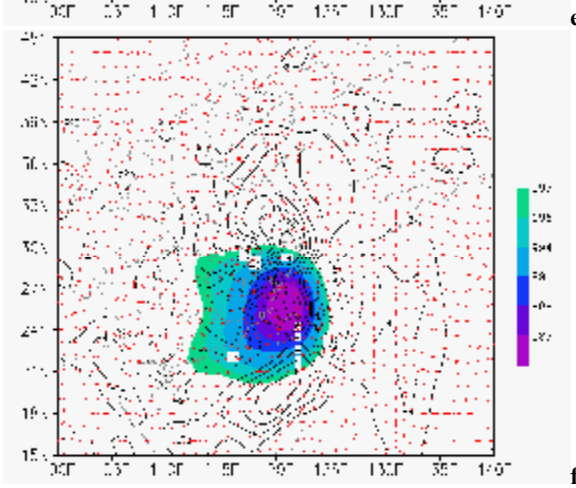
f)

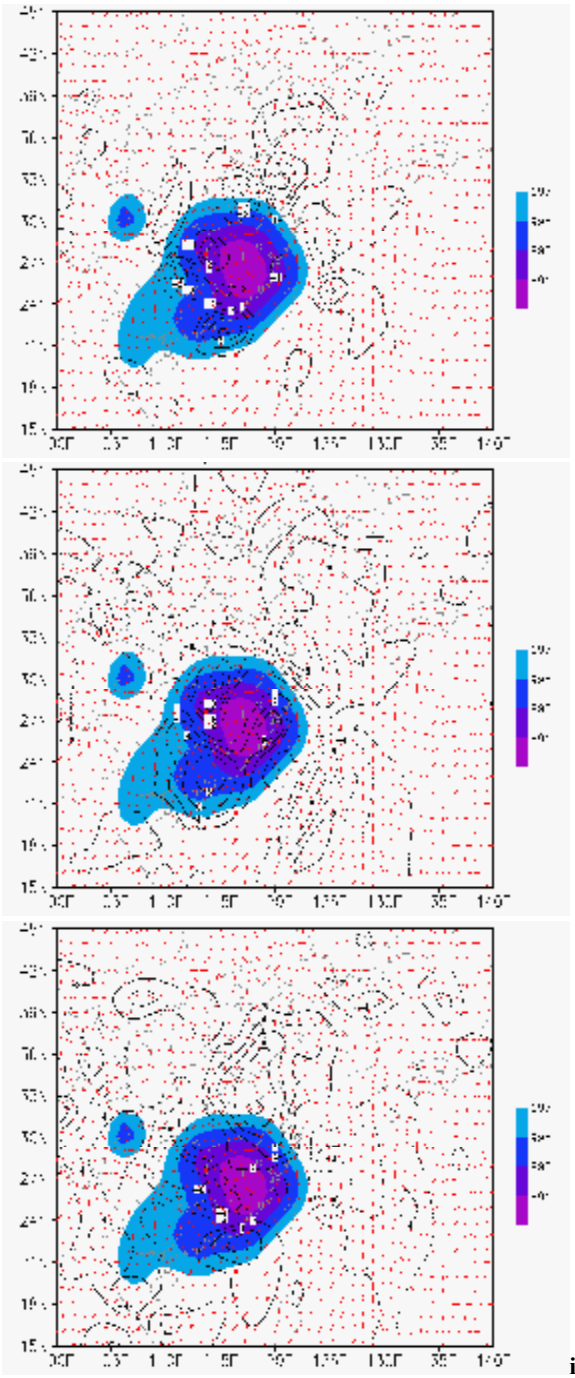

Fig.4 Horizontal distributions on 850 hPa at 1200 UTC 13 (a, b, c), 0000 UTC 14 (d, e, f) and 1200 UTC 14(g, h, i), July 2006 of deformation parameter H_{q_v} (a, d, g, unit: 10^{-13} s^{-2}), stretching deformation η_{q_v} (b, e, h, unit: 10^{-7} s^{-1}) and shear deformation ζ_{q_v} (c, f, i, unit: 10^{-7} s^{-1}). The arrow stands for the horizontal wind vector and the color shade denotes the sea-level pressure. The ordinate is the latitude and the abscissa is the longitude.

3.4 *Dynamic factors influencing the deformation*

To examine the chief dynamic factors responsible for the deformation of moisture flux circulation, the five forcing terms on the RHS of Eq. (11) were calculated and presented in Figs. 5 & 6. As is shown, at 1200 UTC 13 July before landfall, the anomalous areas of the total forcing term (namely, $\langle H_{q_v1}\rangle + \langle H_{q_v2}\rangle + \langle H_{q_v3}\rangle + \langle H_{q_v4}\rangle + \langle H_{q_v5}\rangle$) encircled the low-pressure center of Bilis and the eight positive and negative-valued areas were distributed alternatively. The three forcing terms $\langle H_{q_v1}\rangle$, $\langle H_{q_v2}\rangle$ and $\langle H_{q_v5}\rangle$ were found surrounding the low-pressure center and larger than the $\langle H_{q_v3}\rangle$ and $\langle H_{q_v4}\rangle$ in magnitude. $\langle H_{q_v1}\rangle$ and $\langle H_{q_v2}\rangle$ shared the same spatial phase and their intensities were equivalent. $\langle H_{q_v5}\rangle$ was larger than $\langle H_{q_v1}\rangle$ and $\langle H_{q_v2}\rangle$ in intensity and its spatial phase was almost opposite to that of $\langle H_{q_v1}\rangle$ and $\langle H_{q_v2}\rangle$. But the total forcing term mainly represented the characteristics of $\langle H_{q_v1}\rangle$ and $\langle H_{q_v2}\rangle$. The analysis showed that among the five forcing terms, three terms, namely $\langle H_{q_v1}\rangle$, associated with three-dimensional spatial advection of DP, $\langle H_{q_v2}\rangle$, the difference between squared shear and stretching deformations, coupled with the Coriolis parameter, and $\langle H_{q_v5}\rangle$, the horizontal gradient of geopotential height, made primary contributions to the local change of DP. At 0000 UTC 14 July when Bilis made landfall, the total forcing term was mainly located in the eastern periphery of Bilis and relatively weak in the western periphery. Similar to the situation before landfall, $\langle H_{q_v1}\rangle$, $\langle H_{q_v2}\rangle$, and $\langle H_{q_v5}\rangle$ were chief dynamic forcing factors for DP. Their areas of anomalies appeared at the east periphery of Bilis and were distributed alternatively. The intensity of these anomalies became weaker than before landfall. The spatial phases of $\langle H_{q_v1}\rangle$ and $\langle H_{q_v2}\rangle$ were basically uniform, but opposite to that of $\langle H_{q_v5}\rangle$. At 1200 UTC 14 July when Bilis went deep inland, the total forcing term was further diminished and the alternating distribution pattern of anomalies was destroyed completely (figure omitted). The intensity of $\langle H_{q_v1}\rangle$ was very weak. $\langle H_{q_v5}\rangle$ was opposite to $\langle H_{q_v2}\rangle$ in spatial phase. The intensities of $\langle H_{q_v2}\rangle$ and $\langle H_{q_v5}\rangle$ were still stronger than those of the other three terms, but less intense than before landfall.

The above analysis concerning the dynamic factors impacting the deformation of moisture flux circulation in the periphery of Bilis revealed that before landfall, the chief dynamic factors included three forcing terms, which were associated with the three-dimensional

spatial advection of DP, the difference between shear and stretching deformations, each squared and coupled with the Coriolis parameter, and the horizontal gradient of geopotential height. The first two terms were in the same spatial phase but opposite to the last term in spatial phase. After Bilis went deeper inland, the two terms associated with the Coriolis force and the horizontal gradient of geopotential height made primary contributions to the local change of DP. The two terms with the opposite spatial phase were weakened substantially after landfall.

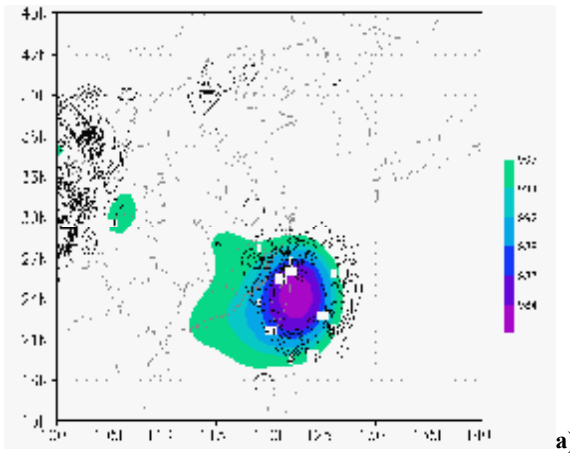
a)

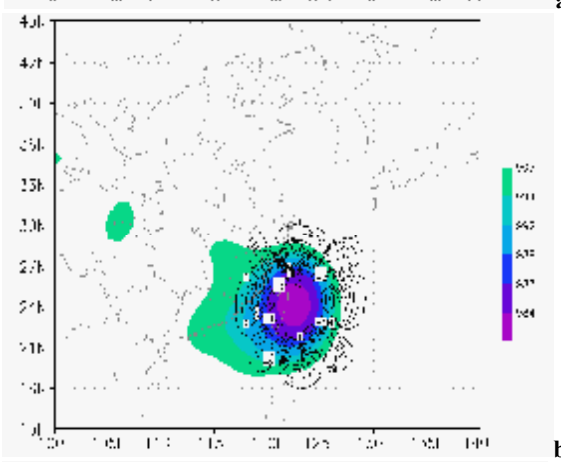
b)

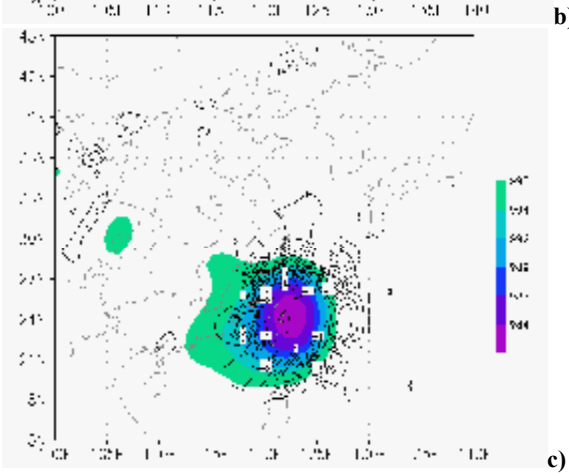
c)

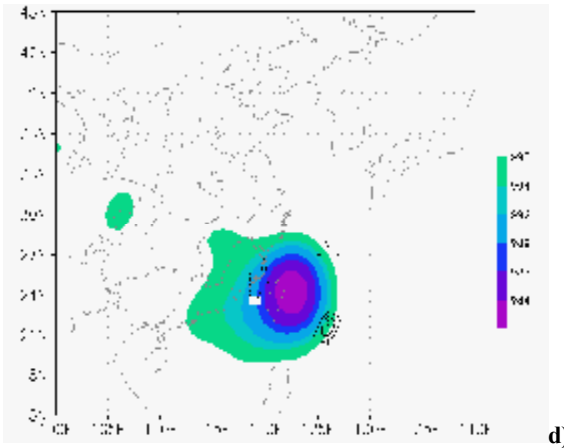
d)

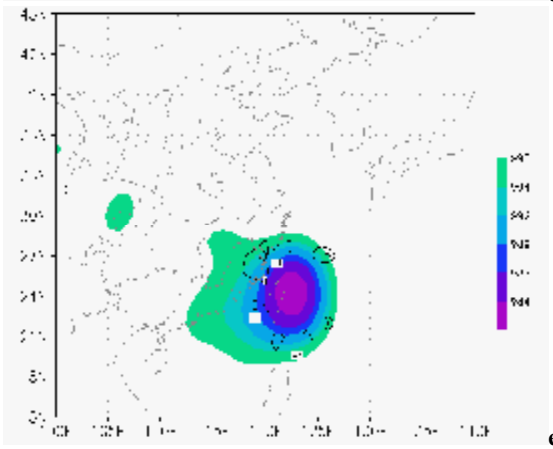
e)

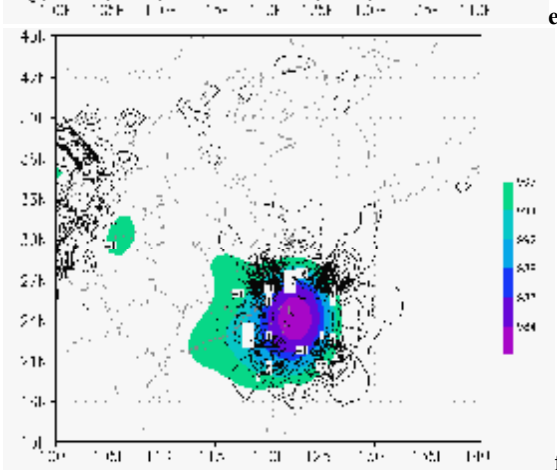
f)

Fig.5 Horizontal distribution of the vertical integrated forcing terms of the tendency equation at 1200 UTC 13 July 2006 (Unit: 10^{-12} Pa s^{-3}) in which a: $\langle H_{q_v 1}\rangle + \langle H_{q_v 2}\rangle + \langle H_{q_v 3}\rangle + \langle H_{q_v 4}\rangle + \langle H_{q_v 5}\rangle$, b: $\langle H_{q_v 1}\rangle$, c: $\langle H_{q_v 2}\rangle$, d: $\langle H_{q_v 3}\rangle$, e: $\langle H_{q_v 4}\rangle$, f: $\langle H_{q_v 5}\rangle$. The color shade denotes the sea-level pressure. The ordinate is the latitude and the abscissa is the longitude.

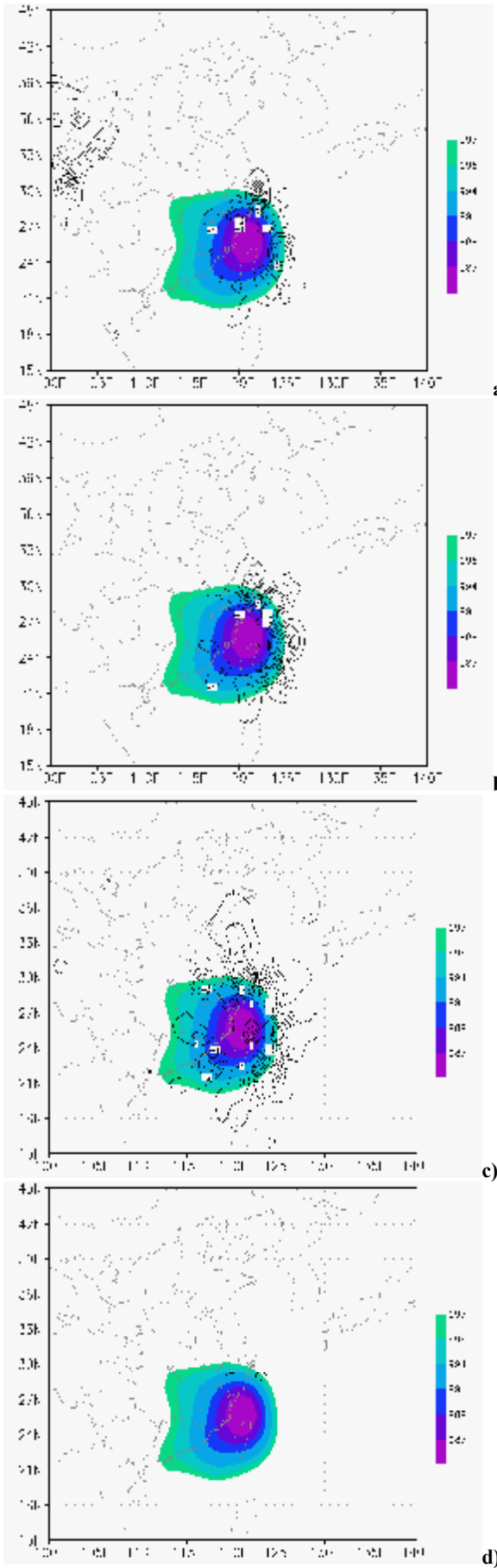

Fig.6 Same as Fig. 5 except at 0000 UTC 14 July 2006.

4 DISCUSSION AND CONCLUSION

Based on the previous theoretical studies about fluid deformation and taking into account the effect of water vapor, we introduce the deformation parameter (DP), which is defined as the product of shear deformation and stretching deformation of the moisture flux circulation. Furthermore, the tendency equation for DP is derived in pressure coordinates. DP is further used to diagnose the deformation character of moisture flux circulation in the periphery of the landfalling Typhoon Bilis. DP and its five forcing terms in the tendency equation are calculated by means of the NCEP/NCAR Global Final Analysis (FNL) dataset, which is used to analyze the temporal and spatial evolutions of DP and the chief dynamic factors impacting DP in the periphery of Bilis.

The analysis showed that before Bilis made landfall, DP had eight anomalous areas that closely surrounded the low-pressure center of Bilis, whose strongly positively valued areas alternated with strongly negative DP areas in horizontal distribution. This indicates that the moisture flux circulation in the periphery of Bilis deformed to rotate counterclockwise and stretch longitudinally and latitudinally before landfall. As Bilis made landfall and further entered

inland China, the moisture flux circulation surrounding the storm adjusted shape gradually from near circularity to ellipse. The intensity of DP decreased accordingly, and the horizontal distribution of coherent zones of DP also became relatively looser. Hence, the deformation of moisture flux circulation in the periphery of Bilis was undermined gradually after landfall. The analysis of vertical and horizontal distributions of DP, stretching deformation, and shear deformation showed that in the vertical cross section, the deformation of moisture flux circulation surrounding Bilis occurred mainly in the middle-lower troposphere and the anomalous areas of shear deformation were in the ½-phase locations of the positive and negative values of stretching deformation. On the horizontal plane (of 850 hPa), there was a $\frac{\pi}{4}$ phase difference between the strongly positive and negative areas of shear deformation and stretching deformation. When Bilis made landfall and went deeper inland, the intensities of DP, shear deformation, and stretching deformation were weakened gradually and their vertical and horizontal structures became loose as well.

The analysis of dynamic factors responsible for the deformation parameter revealed that before landfall, the three terms of three-dimensional spatial advection of DP $\langle H_{q_{v1}} \rangle$, the difference between the squares of shear and stretching deformations coupled with the Coriolis parameter $\langle H_{q_{v2}} \rangle$, and the horizontal gradient of geopotential height $\langle H_{q_{v5}} \rangle$ were the chief dynamic factors impacting the deformation of moisture flux circulation surrounding Bilis. When Bilis made landfall and went farther inland, the chief dynamic factors included the two terms representing (a) the difference between the squares of shear deformation and stretching deformation coupling with the Coriolis parameter $\langle H_{q_{v2}} \rangle$ and (b) the horizontal gradient of geopotential height $\langle H_{q_{v5}} \rangle$. However, compared with the situation before the landfall of Bilis, the intensities of the two forcing terms were greatly weakened.

REFERENCES:

[1] PETTERSSEN S. Weather Analysis and Forecasting [M]. Vol. I, 2nd ed., New York: McGraw-Hill, 1956, 428pp.
[2] YOSHIO K. Atmospheric Dynamics entrance [M]. TIAN Chun-sheng (translator). Beijing: Meteorological Press, 1984, 49pp.
[3] LIU Shi-kuo, LIU Shi-da. Atmospheric Dynamics [M]. Beijing: Peking University Press, 1999.
[4] ZHANG Yuan-jian. Deformation rate and energy front frontogenesis [J]. Acta Meteor. Sinica (in Chinese), 1983, 41(02): 219-222.
[5] DENG Qiu-hua. The deformation field in the planetary boundary layer and heavy rainfall [J]. J. Appl. Meteor. Sci., 1986, 1(02): 165-174.
[6] MARTIN J E. On the Deformation Term in the Quasigeostrophic Omega Equation [J]. Mon. Wea. Rev., 1998, 126: 2000-2007.
[7] WANG Xing-bao, WU Rong-sheng. The development of symmetric disturbances superposed on baroclinic frontal zone under the action of deformation field [J]. Acta Meteor. Sinica (in Chinese), 2000, 58(4): 403-417.
[8] HAN Gui-rong, HE Jin-hai, FAN Yong-fu, et al. The transfiguration frontogenesis analyses on 0108 landfall typhoon extratropical transition and heavy rain structure [J]. Acta Meteor. Sinica (in Chinese), 2005, 63(4): 468-476.
[9] LI D, COLUCCI S. J. The role of deformation and potential vorticity in Southern Hemisphere blocking onsets [J]. J. Atmos. Sci.. 2005, 62: 4043-4056.
[10] LIU Gang, LIU Shi-da, LIU Feng, et al. Vortex dynamics on synoptic maps [J]. Acta Sci. Nat. Univ. Pekin., 2007, 43(1): 17-22.
[11] GAO S, YANG S, XUE M, et al. Total deformation and its role in heavy precipitation events associated with deformation-dominant flow patterns [J]. Adv. Atmos. Sci., 2008, 25: 11-23.
[12] GAO Shou-ting. The foundation and forecasting of mesoscale atmospheric motion [M]. Beijing: Meteorological Press, 2007. 80pp.
[13] PETTERSSEN S, Weather Analysis and Forecasting [M]. 2nd ed, Vol. 1, New York: McGraw-Hill, 1956, 422 pp.

Citation: RAN Ling-kun, YANG Wen-xia and HONG Yan-chao. Deformation of moisture flux circulation surrounding the landfall typhoon "Bilis". *J. Trop. Meteor.*, 2009, 15(2): 167-180.